



CHORUS

This is the accepted manuscript made available via CHORUS. The article has been published as:

Conversion between spin and charge currents with topological insulators

S. Zhang and A. Fert

Phys. Rev. B **94**, 184423 — Published 18 November 2016

DOI: [10.1103/PhysRevB.94.184423](https://doi.org/10.1103/PhysRevB.94.184423)

Conversion between spin and charge currents with topological insulators

S. Zhang¹, and A. Fert²

¹*Department of Physics, University of Arizona, Tucson, AZ 85721 USA*

²*Unité Mixte de Physique, CNRS, Thales, Univ. Paris-Sud,
Université Paris-Saclay, 91767, Palaiseau, France*

Abstract

Injection of a spin current into the surface or interface states of a topological insulator (TI) induces a charge current (Inverse Edelstein Effect or IEE) and, inversely, a charge current flowing at the surface or interface states of a TI generates a non-zero spin density (Edelstein Effect or EE) from which a spin current can be ejected into an adjacent layer. The parameters characterizing the efficiency of these conversions between spin and charge currents have been derived in recent experiments. By using a spinor distribution function for a momentum-spin locked TI, we determine a number of spin transport properties of TI-based heterostructure and find that the spin to charge conversion in IEE is controlled by the relaxation of an out-of equilibrium distribution in the TI states while the charge to spin conversion in EE depends on the electron transmission rate at the interface of the TI.

PACS numbers: 72.25.-b, 73.40.-c, 72.25.Mk

The electronic states of the two-dimensional electron gas (2DEG) at the surfaces or interfaces of the topological insulators^{1,2} are characterized by dispersion surfaces of Dirac cone type and Fermi contours with helical locking of the spin with the momentum by spin-orbit coupling, as shown in Fig.1a (for simplicity we will assume a simple circular Fermi contour throughout the letter). This locking between spin and momentum enables the conversion between spin and charge currents by the Edelstein (EE) and Inverse Edelstein (IEE) effects³⁻⁵, see Fig.1b-d. In EE a charge current in the 2DEG, i.e. a shift of the Fermi contours in the direction x of the electron motion, induces an overpopulation of spins in the transverse (y) direction due to spin-momentum locking, and therefore is associated with a nonzero spin density (spin accumulation). The spin accumulation can diffuse through an interface into an adjacent conducting material, resulting in a pure 3D spin current injected into this material, without a net charge flow. In the inverse conversion by IEE the injection of a spin current into the TI induces a charge current in the 2DEG at its surface or interface. As shown by series of recent experiments⁶⁻¹⁰ using TI, the conversion between spin and charge by EE and IEE is remarkably efficient and very promising for the creation or detection of spin currents in spintronic devices. In experiments of spin pumping, for example, a spin current generated by the ferromagnetic resonance of a magnetic layer is injected through a thin metallic layer into the surface or interface state of a TI and converted by IEE into a 2-dimensional (2D) charge current. Such conversions by IEE are characterized by the length λ_{IEE} that was first introduced for Rashba interfaces^{4,5}, and defined as the ratio between the induced 2D-charge current density \mathbf{J}_c and the injected 3D-spin current density \mathbf{J}_s . The IEE length has been predicted¹⁰ in a phenomenological model to be expressed as

$$\lambda_{IEE} \equiv \left| \frac{\mathbf{J}_c}{\mathbf{J}_s} \right| = v_F \tau_{IEE} \quad (1)$$

where v_F is the Fermi velocity on the Dirac cone and τ_{IEE} is defined as the relaxation time of an out-of-equilibrium distribution of the topological 2D states (here we focus on the absolute value of IEE; the directions of the induced charge current relative to the spin current has been defined and discussed in Ref.¹⁰). In the same way the conversion between 2D charge current into 3D spin currents by EE can be characterized by the parameter q_{EE} (an inverse of length, q_{ICS} in the notation of Kondou *et al.*⁷),

$$q_{EE} \equiv \left| \frac{\mathbf{J}_s}{\mathbf{J}_c} \right| = \frac{1}{v_F \tau_{EE}} \quad (2)$$

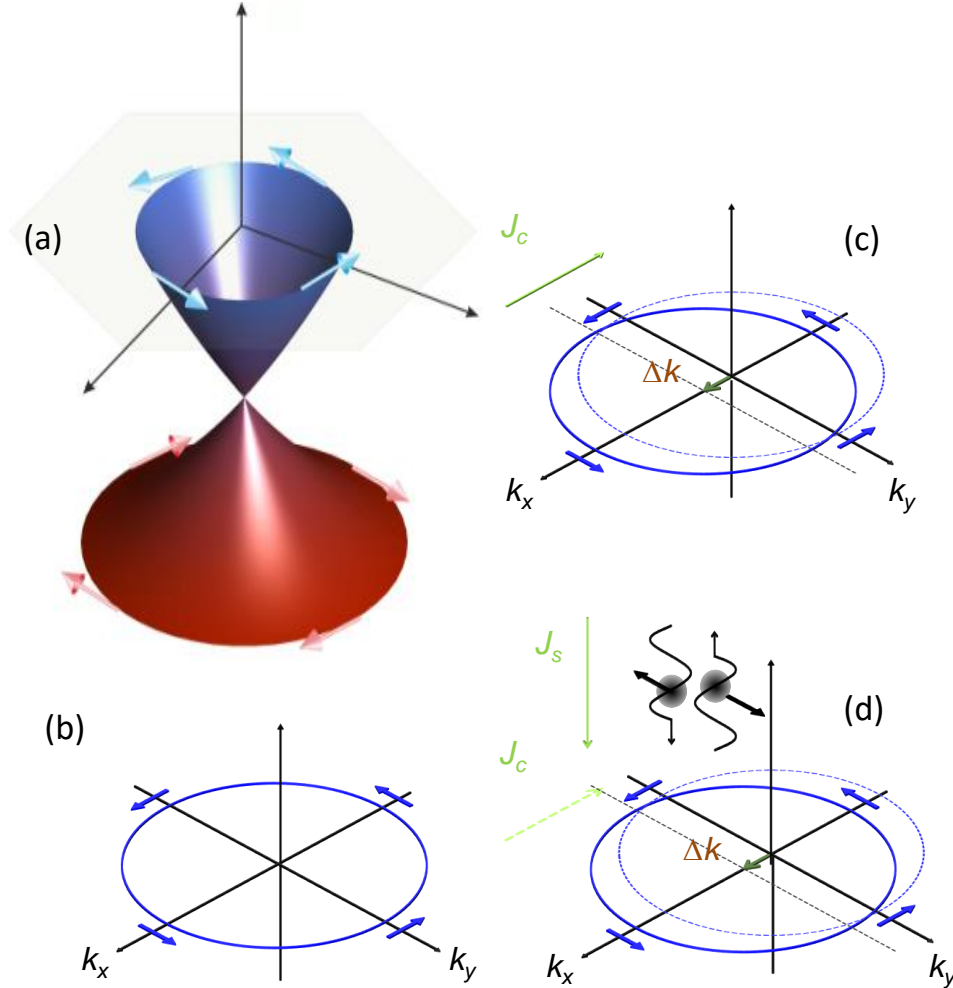


FIG. 1: (Color Online) Schematically shown of (a,b) Dirac cone dispersion and Fermi contour with spin-momentum locking of surface/interface states of topological insulator. (c) Edelstein Effect (EE): an charge current \mathbf{J}_c along $-x$ generates a nonzero spin density along y (spin accumulation). (d): Vertical injection of a spin current (wiggled lines with spin-polarization along y) generates a charge current along $-x$ ¹¹

Several theoretical approaches^{5,12} have been developed to address the spin-charge conversion by TI and focused on the precessional motion of electron spins if the spin direction of the injected electrons is *not* perpendicular to the momentum of the TI states. In this case, the injected electron is not an eigenstate of the TI and the dephasing takes place for the non-equilibrium electron spin injected in the TI. The spin-charge conversion comes from a

subtle and detailed balance among spin injection, spin precession and spin relaxation.

In this paper, we provide a theory that determines the key physical parameters controlling τ_{IEE} and τ_{EE} of Eqs. (1) and (2). To display the most physically transparent picture in the spin-to-charge conversion, we limit the calculation to the simple case of predominant contribution of surface states on a Dirac cone with helical in-plane locking. In general, some mixture of surface and bulk states can take place around the Fermi level when a metallic overlayer is in contact with the TI. Consequently, the surface states are altered by the Fermi level shift, band-bending and possible creation of additional surface states. It has been shown that the spin-momentum locked surface states could be completely destroyed by a magnetic overlayer¹³. However our simplifying model is most useful in addressing the most recent experimental results in which the predominant contribution to spin-charge conversion can be attributed to Dirac cone 2D states. We refer to the two following examples: a) Thin films of α -Sn present Dirac cone in a large gap of 1.2 eV for 44 atomic layers with the Dirac point at about the middle of the gap (see Fig.2 in¹⁴). In contact with Ag and from ARPES measurements, the Dirac cone is still observed and the Fermi level is at 0.65 meV above the Dirac point, whereas the contact with Fe destroys the Dirac cone¹⁰. b) For Bi_2Se_3 and $(\text{Bi,Sb})_2\text{Se}_3$, it is clearly demonstrated by Wang *et al.*¹⁵ in which conditions a predominant 2D contribution can be obtained.

We start with defining the wavefunction of the TI surface states as $\psi_{\mathbf{p}}(\boldsymbol{\rho})\chi_{\mathbf{p}}$ where \mathbf{p} denotes the momentum at the 2D surface, $\boldsymbol{\rho} = (x, y)$ is the position, $\psi_{\mathbf{p}}$ is the orbital part of the wavefunction and $\chi_{\mathbf{p}}$ is the spin part which is perpendicular to the \mathbf{p} , i.e., $\boldsymbol{\sigma} \cdot (\hat{\mathbf{z}} \times \hat{\mathbf{p}})\chi_{\mathbf{p}} = \chi_{\mathbf{p}}$ where $\boldsymbol{\sigma}$ is the Pauli matrix vector, $\hat{\mathbf{z}}$ is the unit vector normal to the surface, and $\hat{\mathbf{p}} = \mathbf{p}/p$ is the unit vector for the direction of the momentum. Since the spin quantization axis for a given \mathbf{p} is $\hat{\mathbf{z}} \times \hat{\mathbf{p}}$, the Boltzmann distribution must take the following spinor form,

$$\hat{g}_{\mathbf{p}} = g_c(\mathbf{p}) + g_s(\mathbf{p})\boldsymbol{\sigma} \cdot (\hat{\mathbf{z}} \times \hat{\mathbf{p}}) \quad (3)$$

where g_c and g_s are spin-independent and spin-dependent parts. We recall that, in ferromagnetic conductors, the spinor is of the form $\boldsymbol{\sigma} \cdot \mathbf{M}$ where \mathbf{M} is the local magnetization; while for non-magnetic metals (NM), the polarization is not given *a priori* and one writes an unspecified spinor $\boldsymbol{\sigma} \cdot \mathbf{A}$ where the vector \mathbf{A} could be any direction to be self-consistently determined by boundary conditions. The spinor form given in Eq. (3) is unique to the spin-momentum locked band structure. We next determine the distribution function in Eq. (3)

for a bilayer made of a NM layer and the TI (as in the experiments of^{7,9}). The spinor Boltzmann equation reads,

$$\frac{d\hat{g}_{\mathbf{p}}}{dt} = \sum_{\mathbf{k}} \Gamma_{\mathbf{k}\mathbf{p}}(\hat{f}_{\mathbf{k}} - \hat{g}_{\mathbf{p}}) + \sum_{\mathbf{p}'} \Delta_{\mathbf{p}\mathbf{p}'}(\hat{g}_{\mathbf{p}'} - \hat{g}_{\mathbf{p}}) \quad (4)$$

where $\hat{f}_{\mathbf{k}}$ is the distribution function in the non-magnetic metal, $\Gamma_{\mathbf{k}\mathbf{p}}$ is the transition rate across the interface between the state \mathbf{k} in the NM and the state \mathbf{p} in the TI, $\Delta_{\mathbf{p}\mathbf{p}'}$ is the (defect or impurity) scattering probability between states \mathbf{p} and \mathbf{p}' in the TI. In the following, we determine the spin and momentum dependence of these parameters in Eq. (4).

The transition probability $\Gamma_{\mathbf{k}\mathbf{p}}$ at the interface is

$$\Gamma_{\mathbf{k}\mathbf{p}} = | \langle \psi_{\mathbf{k}\sigma} | V(\mathbf{r}) | \psi_{\mathbf{p}} \chi_{\mathbf{p}} \rangle |^2 \delta(\epsilon_{\mathbf{k}} - \epsilon_{\mathbf{p}}) \quad (5)$$

where $\psi_{\mathbf{k}\sigma}$ is the wavefunction of the NM layer, and $V(\mathbf{r})$ is the step-like interface potential. For the NM metal, the orbital part of the wavefunction is independent of spin, i.e., $\psi_{\mathbf{k}\sigma} = \psi_{\mathbf{k}} \chi_{\sigma}$. If we further assume that the interface potential is spin-independent and the interface is rough enough so that the momentum conservation across the interface does not apply, the above scattering matrix takes the following simple form

$$\Gamma_{\mathbf{k}\mathbf{p}} = [1 + \boldsymbol{\sigma} \cdot (\hat{\mathbf{z}} \times \hat{\mathbf{p}})] / \tau_t \quad (6)$$

where τ_t characterizes the tunneling time across the interface (the inverse of the transition probability). Note that the dependence of the spin and momentum in the transition probability is solely from the spin-momentum locking of the TI states: the probability is highest if the spin of the \mathbf{k} state is parallel to $\hat{\mathbf{z}} \times \hat{\mathbf{p}}$ and is zero if antiparallel.

The defect or impurity scattering rate between the states \mathbf{p} and \mathbf{p}' of the TI is

$$\Delta_{\mathbf{p}\mathbf{p}'} = | \langle \psi_{\mathbf{p}'} \chi_{\mathbf{p}'} | V_{sc}(\boldsymbol{\rho}) | \psi_{\mathbf{p}} \chi_{\mathbf{p}} \rangle |^2 \delta(\epsilon_{\mathbf{p}} - \epsilon_{\mathbf{p}'}) \quad (7)$$

where $V_{sc}(\boldsymbol{\rho})$ is the scattering potential of the impurities or defects. If the scattering potential is short-ranged and spin-independent, the above scattering reduces to

$$\Delta_{\mathbf{p}\mathbf{p}'} = (1 + \hat{\mathbf{p}} \cdot \hat{\mathbf{p}'}) / \tau_p \quad (8)$$

where we have introduced a relaxation time τ_p to represent the strength of the scattering within the TI band. The momentum dependence again comes from the spin momentum

locking. If the momenta are antiparallel, $\hat{\mathbf{p}}' = -\hat{\mathbf{p}}$, the scattering amplitude vanishes—this is known as zero backscattering for the TI. However, as long as they are not antiparallel, any impurity scattering contains spin-flip processes.

Next we define the spin chemical potential $\boldsymbol{\mu} \equiv (eN_F)^{-1} \sum_{\mathbf{k}} \text{Tr}_{\sigma}(\boldsymbol{\sigma} \hat{f}_{\mathbf{k}})$, where e is the electron charge and N_F is the density of states of the NM at the Fermi level. Note that the electron hopping from the NM to the TI occurs at the interface, thus N_F is the density state *projected* on the 2D surface, i.e., the unit of N_F is the inverse of the energy *per area* which is approximately the product of the 3d density states and the interface layer thickness (lattice constant). By using Eqs. (6) and (8), we find that, for the steady state solution of Eq. (4) $d\hat{g}_{\mathbf{p}}/dt = 0$, can be obtained exactly

$$\hat{g}_{\mathbf{p}} = \frac{2e\tau_p N_F}{4\tau_p + \tau_t} \boldsymbol{\mu} \cdot (\hat{\mathbf{z}} \times \hat{\mathbf{p}}) [1 + \boldsymbol{\sigma} \cdot (\hat{\mathbf{z}} \times \hat{\mathbf{p}})]. \quad (9)$$

We can immediately evaluate the spin accumulation in the TI

$$\delta \mathbf{m} = \sum_{\mathbf{p}} \text{Tr}_{\sigma}(\mu_B \boldsymbol{\sigma} \hat{g}_{\mathbf{p}}) = \frac{\mu_B \tau_p N_F}{4\tau_p + \tau_t} \boldsymbol{\mu} \quad (10)$$

where μ_B is the Bohr magneton, and the charge current in the TI is then

$$\mathbf{J}_c = \sum_{\mathbf{p}} \text{Tr}_{\sigma}(e\mathbf{v} \hat{g}_{\mathbf{p}}) = \frac{e^2 \tau_p v_F N_F}{4\tau_p + \tau_t} (\boldsymbol{\mu} \times \hat{\mathbf{z}}) \quad (11)$$

where e is the electron charge and v_F is the Fermi velocity. Note that the spin current in the TI is zero, i.e., $\text{Tr}_{\sigma} \sum_{\mathbf{p}} (\boldsymbol{\sigma} \mathbf{v} \hat{g}_{\mathbf{p}}) = 0$. The spin current across the interface, on the other hand, can be readily identifies as the summation over the first term (times the spin matrix) in Eq. (4),

$$\mathbf{J}_s = \sum_{\mathbf{k}\mathbf{p}} \text{Tr} \left[e \boldsymbol{\sigma} \Gamma_{\mathbf{k}\mathbf{p}} (\hat{f}_{\mathbf{k}} - \hat{g}_{\mathbf{p}}) \right] = \frac{e^2 N_F}{4\tau_p + \tau_t} \boldsymbol{\mu} \quad (12)$$

Thus, the spin to charge conversion rate is

$$\lambda_{IEE} = \frac{|\mathbf{J}_c|}{|\mathbf{J}_s|} = v_F \tau_p \equiv \lambda_{mf}, \quad (13)$$

i.e., the IEE length is exactly the mean free path of the TI, which has been proposed earlier in the interpretation of experiments, see Eq. (1). At first, one might be surprised by this result since the spin-independent defect or impurity scattering by itself does not involve spin-flip. However, the spin-momentum locked TI band transfers any momentum scattering to spin rotation. We also want to emphasize that the IEE length derived here comes from

scattering within the TI band, while the other scatterings, particularly those due also to the hybridization of the TI with bulk states (in the TI bulk as well as in the NM), could significantly contribute the IEE length as well through an additional contribution to τ_p .

Experimentally, the charge current can be directly measured while the spin current entering the TI can be obtained via the enhanced FMR linewidth broadening. To determine the absolute values of charge/spin currents from Eq. (11) and (12), we consider a typical trilayer consisting of FM/NM/TI where the FM stands for a conventional ferromagnet such as NiFe. The spin pumping by the precession of the FM layer leads to a spin current across the FM/NM interface¹⁶,

$$\mathbf{J}_s = \frac{eG_{mix}}{\pi\hbar} \left(\frac{\hbar}{2} \mathbf{m} \times \frac{d\mathbf{m}}{dt} - e\boldsymbol{\mu} \right) \quad (14)$$

where G_{mix} is the mixing conductance of the FM/NM interface, \mathbf{m} is the unit vector in the direction of the magnetization of the FM layer. The chemical potential at the FM/NM would exponentially decay when electrons diffuse across the NM layer. However, if the thickness of the NM layer is much smaller than the spin-diffusion length, we may simply assume that the chemical potential maintains a constant throughout the NM layer and thus we may equate Eq. (12) and (14), and find

$$\mathbf{J}_s = \frac{e}{2\pi} \left(\frac{1}{G_{mix}} + \frac{1}{G_t} + \frac{4}{G_p} \right)^{-1} \mathbf{m} \times \frac{d\mathbf{m}}{dt} \quad (15)$$

where $G_p = \pi\hbar N_F \tau_p^{-1}$ and $G_t = \pi\hbar N_F \tau_t^{-1}$.

Up till now, we have considered transition probabilities among eigenstates of the NM and TI, i.e., the electron spins injected to the TI layer is to change the *non-equilibrium occupation number* without altering the electronic states of the TI. However, if the electron spin injected into the TI is not a spin eigenstate of the TI, a spin torque will be applied to the spins of the TI. We recall the spin injection from a NM layer to a ferromagnetic layer in which a spin torque on the magnetization in the form of $\mathbf{m} \times (\mathbf{m} \times \mathbf{J}_s)$ ¹⁷ could rotate the magnetization and possibly creates a dynamic procession of the FM layer if the spin torque is strong enough. In the TI, an electron spin with a given momentum \mathbf{p} receives a torque $\boldsymbol{\tau} = \mathbf{s} \times (\mathbf{s} \times \mathbf{J}_s)$ so that the total torque satisfies,

$$\frac{d\mathbf{s}}{dt} = -\alpha\gamma_0 \mathbf{s} \times (\hat{\mathbf{z}} \times \hat{\mathbf{p}}) + \mathbf{s} \times (\mathbf{s} \times \mathbf{J}_s) \quad (16)$$

where γ_0 is the gyro magnetic ratio, α is the spin-orbit coupling strength of the TI (or the spin-orbit locking strength). Since the spin chemical potential is very small compared to the

spin-orbit coupling (α) of the TI, the steady state $ds/dt = 0$ solution of Eq. (16), up to the first order in J_s/α , is

$$\delta\mathbf{s} \equiv \mathbf{s} - \hat{\mathbf{z}} \times \hat{\mathbf{p}} = \frac{\mathbf{J}_s}{\alpha\gamma_0} \times (\hat{\mathbf{z}} \times \hat{\mathbf{p}}). \quad (17)$$

If \mathbf{J}_s is polarized in the plane of the layer, say $\mathbf{J}_s = J_s\hat{\mathbf{y}}$, an out-of-equilibrium spin component $\delta s_z = (p_y/p_F)(J_s/\alpha\gamma_0)$ has been induced due to the absorption of the spin current by the TI; this spin component has also been obtained in Ref.^{5,12}. The effect of this spin torque is negligibly small on the spin dynamics of the TI because α is much larger than the spin current induced torque—this is in sharp difference from the spin injection to a FM in which the resulting spin torque is competing with a much smaller energy scale (such as the anisotropy and the applied magnetic field) and it could excite magnetization switching and precessing¹⁸.

One of the consequences of the above induced out-of-plane component is an unusual spin Hall current¹⁹: a z-component spin polarization and y-direction of the electron flow \mathbf{J}_y^z . Recall the definition $J_y^z = \sum_{\mathbf{p}} \text{Tr}(v_y s_z \hat{g}_{\mathbf{p}})$, we find $J_y^z = v_F J_s / \alpha\gamma_0$ where we use s_z given above and *equilibrium* distribution function $\hat{g}^{(0)}$.

We now turn to the inverse effect: an applied charge current in the TI produces a spin current in the NM layer. Consider a bilayer TI/NM with a semi-infinite NM layer. The distribution function at the interface of the NM layer $\hat{f}_{\mathbf{k}}$ satisfies,

$$\frac{d\hat{f}_{\mathbf{k}}}{dt} = \sum_{\mathbf{p}} \Gamma_{\mathbf{p}\mathbf{k}} (\hat{g}_{\mathbf{p}} - \hat{f}_{\mathbf{k}}) - \frac{\hat{f}_{\mathbf{k}} - (\hat{I}/2)\text{Tr}\hat{f}_{\mathbf{k}}}{\tau_{sf}} \quad (18)$$

where \hat{I} is the 2×2 unit matrix and τ_{sf} is the spin-flip scattering time in the NM. For a given charge density in the TI layer, $\mathbf{J}_c \equiv \sum_{\mathbf{p}} \text{Tr}(e v_{\mathbf{p}} g_{\mathbf{p}})$ where $g_{\mathbf{p}} \propto p_x [1 + \boldsymbol{\sigma} \cdot (\hat{\mathbf{z}} \times \hat{\mathbf{p}})]$, we can readily obtain the $\hat{f}_{\mathbf{k}}$, in the steady state case, the spin current across the NM/TI interface,

$$\mathbf{J}_s = \frac{1}{v_F(\tau_t + \tau_{sf})} \hat{\mathbf{z}} \times \mathbf{J}_c, \quad (19)$$

Thus, $q_{EE} \equiv |\mathbf{J}_s/\mathbf{J}_c| = [v_F(\tau_t + \tau_{sf})]^{-1}$. The charge to spin current inversion rate depends on the spin flip rate in the NM metal and the transition rate at the NM/TI interface, but independent of the impurity scattering of the TI layer. If $\tau_{sf} \rightarrow \infty$, i.e., no spin absorption in the NM layer, the spin current flows back to in the TI, leading to zero net spin current. Similarly, when $\tau_t \rightarrow \infty$, i.e., no transition across the interface, the spin current obviously disappears since the interface blocks the electron flow. The relaxation time τ_p is not involved in q_{EE} , but only in the resistivity of the 2DEG: a long τ_p would generate proportionally large

\mathbf{J}_c and \mathbf{J}_s for a given applied voltage. In some experiments^{6,7}, the spin current is measured via the spin torque where a ferromagnetic layer (FM) is placed on the other side of the NM layer. In this case, if we assume that the NM layer is much thinner than the spin diffusion length, the distribution in the NM layer is now determined by

$$\frac{d\hat{f}_{\mathbf{k}}}{dt} = \sum_{\mathbf{p}} \Gamma_{\mathbf{p}\mathbf{k}}(\hat{g}_{\mathbf{p}} - \hat{f}_{\mathbf{k}}) - \frac{G_{mix}}{\pi\hbar N_F} \hat{f}_{\mathbf{k}} \quad (20)$$

where the last term represents the flow of the spin current from the NM to the FM layer if the magnetization of the FM is oriented perpendicularly to the spin current. Thus, we obtain,

$$q_{EE}^{-1} = \pi\hbar N_F v_F \left(\frac{1}{G_t} + \frac{1}{G_{mix}} \right). \quad (21)$$

If the spin current is not perpendicular to the FM, it will penetrate into the FM to be partially relaxed inside the FM and partially reflected (back flow), thus reducing the spin current.

Finally, we compare our theoretical predictions with experimental results on the conversion between spin and charge currents.

For the conversion from spin to charge by IEE, we first consider the example of spin pumping from an Fe layer into the topological insulator α -Sn through a thin Ag layer¹⁰. With spin-momentum locked 2D states at Ag/Sn interfaces characterized by a quasi-circular Fermi contour and the Fermi velocity $v_F = 5.6 \times 10^5$ m/s, we can account for the experimental value of $\lambda_{IEE} = 2.1$ nm by our Eq. (13) with $\tau_p = 3.7$ fs, as also found in¹⁰. This relatively short relaxation time is in the same range as the IEE relaxation time found in spin pumping experiments on Rashba 2DEGs where $\tau_p = 5$ fs for Bi/Ag Rashba interfaces⁴ and the relaxation time derived from optical measurement on 2D states at interfaces between metals²⁰. It has been argued by Rojas-Sanchez *et al.*¹⁰ that such relatively short relaxation times at interfaces with metals can be due to additional relaxation mechanisms coming from the hybridization of the 2D states with metallic 3D states; this is consistent with the much longer τ_p (in the range of picosecond) derived for the IEE relaxation time of the 2DEG at the interface between the LAO and STO insulating oxides²¹. Further experiments on TI protected by insulating materials would be of interest to see if the effective IEE time and the efficiency of the conversion can be enhanced in heterostructures without TI/metal interfaces.

It is also interesting to compare the prediction of Eq.(15) for the effective spin mixing conductance, $G_{mix}^* \equiv (1/G_{mix} + 1/G_t + 1/G_p)^{-1}$, that can be derived from the broadening of the FMR line width in experiments of spin pumping into TI. It has been found experimentally that G_{mix}^* for spin pumping from Fe through Ag into α -Sn ($G_{mix}^* = 40/nm^2$), as well as spin pumping into Bi_2Se_3 from CoFeB ($G_{mix}^* = 12 - 260/nm^{222}$) or NiFe ($G_{mix}^* = 42/nm^{223}$), is always in the range of the spin mixing conductance in purely metallic systems ($G_{mix} = 40/nm^2$ at the Co/Pt interface²⁴). Clearly, both G_t and G_p should not be smaller than G_{mix} of FM/NM systems in order to retain G_{mix}^* comparable to G_{mix} . As G_t is the mixing conductance of NM/TI interface, it would be comparable to G_{mix} if both interfaces have similar quality. For G_p , we can estimate by using $\tau_p = 3.7fs$ and $N_F = 2$ ($eV \text{ \AA}^2$)⁻¹ (for a free electron model of a metal as Ag), yielding $G_p = 100/nm^2$ which is indeed the same order as G_{mix} .

For the conversion from charge to spin, the order of magnitude of the experimental results is also consistent with Eq. (21). Considering the results on the conversion from a spin current in $(Bi_{1-x}Sb_x)_2Te_3$ series of TI to a spin current injected in NiFe through Cu⁷, if we also suppose that both G_t at the TI/Cu interface and G_{mix} at the Cu/NiFe interface are of the order of 100 nm^{-2} and assume the same value of N_F for Cu and Ag with v_F around $3.7 \times 10^5 \text{ m/s}^7$, one obtains $\mathbf{q}_{EE} \approx 0.3nm^{-1}$, not very far from the experimental results in Ref.⁷ between 0.4 and 1.1 nm^{-1} (except in the vicinity of the Dirac point⁷).

In summary we used the spinor distribution function for momentum-spin locked states to derive the main parameters involved in spin-charge conversion by TI. In particular, we find that the spin to charge conversion is related to the relaxation of the topological states whereas the opposite conversion depends essentially on interface parameters, in contrast with the description of similar conversions with spin Hall effect where a single parameter, the spin Hall angle, characterizes both conversions. Our results can be a useful guide for the exploitation of TI in spintronics.

S. Z. thanks the CNRS/Thales laboratory in Palaiseau for its hospitality. This work is supported by a public grant overseen by the French National Research Agency (ANR) as part of the Investissements d'Avenir program (Labex NanoSaclay, reference: ANR-10-LABX-

0035) and is also partially supported by NSF-ECCS-1404542 (SZ).

- ¹ B. A. Bernevig, T. L. Hughes, and S. -C. Zhang, *Science* **314**, 17571761 (2006).
- ² M. Z Hasan and C. L. Kane, *Rev. Mod. Phys.* **82**, 30453067 (2010).
- ³ V. M. Edelstein, *Solid State Commun.* **73**, 233235 (1990).
- ⁴ J. C. Rojas-Sanchez, L. Vila, G. Desfonds, S. Gambarelli, J. P. Attané, J. M. De Teresa, C. Magén, and A. Fert, *Nat. Commun.* **4**, 2944 (2013).
- ⁵ K. Shen, G. Vignale, and R. Raimondi, *Phys. Rev. Lett.* **112**, 096601 (2014).
- ⁶ A. R. Mellnik, J. S. Lee, A. Richardella, J. L. Grab, P. J. Mintun, M. H. Fischer, A. Vaezi, A. Manchon, E. A. Kim, N. Samarth, D. and C. Ralph, *Nature* **511**, 449 (2014).
- ⁷ K. Kondou, R. Yoshimi, A. Tsukazaki, Y. Fukuma, J. Matsuno, K. S. Takahashi, M. Kawasaki, Y. Tokura and Y. Otani, *Nature Physics*, doi:10.1038/nphys3833 (2016).
- ⁸ J. Tian, I. Miotkowski, S. Hong, and Y. P. Chen, *Sci. Rep.* **5**, 14293 (2015).
- ⁹ Y. Shiomi, K. Nomura, Y. Kajiwara, K. Eto, M. Novak, Kouji Segawa, Yoichi Ando, and E. Saitoh, *Phys. Rev. Lett.* **113**, 196601 (2014).
- ¹⁰ J.-C. Rojas-Sanchez, S. Oyarzn, Y. Fu, A. Marty, C. Vergnaud, S. Gambarelli, L. Vila, M. Jamet, Y. Ohtsubo, A. Taleb-Ibrahimi, P. Le Fvre, F. Bertran, N. Reyren, J.-M. George, and A. Fert, *Phys. Rev. Lett.* **116**, 096602 (2016).
- ¹¹ We thank S. Valenzuela and N. Reyren for drawing the Fig. 1.
- ¹² Xin Liu and Jairo Sinova, *Phys. Rev. Lett.* **111**, 166801 (2013).
- ¹³ Jia Zhang, Julian P. Velez, Xiaoqian Dang, and Evgeny Y. Tsymbal, *Phys. Rev. B* **94**, 014435 (2016).
- ¹⁴ S. Kufner, M. Fitzner, and F. Bechstedt *Phys. Rev. B* **90**, 125312 (2014).
- ¹⁵ Hailong Wang, James Kally, Joon Sue Lee, Tao Liu, Houchen Chang, Danielle Reifsnnyder Hickey, K. Andre Mkhoyan, Mingzhong Wu, Anthony Richardella, and Nitin Samarth, *Phys. Rev. Lett.* **117**, 076601 (2016).
- ¹⁶ Y. Tserkovnyak, A. Brataas, and G. E. W. Bauer, *Phys. Rev. Lett.* **88**, 117601 (2002).
- ¹⁷ J. C. Slonczewski, *J. Mag. Mag. Mater.* **159**, L1 (1996).
- ¹⁸ J. A. Katine, F. J. Albert, R. A. Buhrman, E. B. Myers, and D. C. Ralph *Phys. Rev. Lett.* **84**, 3149 (2000).

- ¹⁹ J. E. Hirsch, Phys. Rev. Lett. **83**, 1834 (1999).
- ²⁰ S.Ogawa, H. Nagano, and H. Petek, Phys. Rev. Lett. **88**, 116801 (2002).
- ²¹ E. Lesne, Yu Fu, S. Oyarzun, J. C. Rojas-Snchez, D. C. Vaz, H. Naganuma, G. Sicoli, J.-P. Attane, M. Jamet, E. Jacquet, J.-M. George, A. Barthelemy, H. Jaffres, A. Fert, M. Bibes, and L. Vila, Nature Materials, DOI: 10.1038/nmat4726 (2016).
- ²² Mahdi Jamali, Joon Sue Lee, Jong Seok Jeong, Farzad Mahfouzi, Yang Lv, Zhengyang Zhao, Branislav K. Nikolic, K. Andre Mkhoyan, Nitin Samarth, and Jian-Ping Wang, Nano Lett., **15**, 7126 (2015).
- ²³ A. A. Baker, A. I. Figueroa, L. J. Collins-McIntyre, G. van der Laan, and T. Hesjedala, Scientific Reports **5**, 7907 (2015).
- ²⁴ J.-C. Rojas-Snchez, N. Reyren, P. Laczkowski, W. Savero, J.-P. Attan, C. Deranlot, M. Jamet, J.-M. George, L. Vila, and H. Jaffres, Phys. Rev. Lett. **112**, 106602 (2014).